Scopes, R. K. (1974) *Anal. Biochem. 59*, 277-282.
Smith, D. L., Almo, S. C., Toney, M. D., & Ringe, D. (1989) *Biochemistry 28*, 8161-8167.
Sung, M., Tanizawa, K., Tanaka, H., Kuramitsu, S., Kagamiyama, H., Hirotsu, K., Okamoto, A., Higuchi, T., & Soda, K. (1991) *J. Biol. Chem. 266*, 2567-2572.
Toney, M. D., & Kirsch, J. F. (1987) *J. Biol. Chem. 262*, 12403-12405.
Toney, M. D., & Kirsch, J. F. (1989) *Science 243*, 1485-1488.
Velick, S. F., & Vavra, J. (1962) *J. Biol. Chem. 237*, 2109-2122.
Wells, J. A. (1990) *Biochemistry 29*, 8509-8517.

The Rate of Formation of Transition-State Analogues in the Active Site of Adenosine Deaminase Is Encounter-Controlled: Implications for the Mechanism†

Linda C. Kurz,* Luke Moix, Marian C. Riley, and Carl Frieden
Department of Biochemistry and Molecular Biophysics, Division of Biology and Biomedical Sciences, Washington University School of Medicine, St. Louis, Missouri 63110

Received June 3, 1991; Revised Manuscript Received August 29, 1991

ABSTRACT: We have previously shown that purine riboside, when bound to adenosine deaminase, forms a complex in which C-6 of the purine is tetrahedral [Kurz, L. C., & Frieden, C. (1987) *Biochemistry 26*, 8450]. We now report the rates of formation of enzyme–inhibitor complexes of two types, those which do and those which do not form such tetrahedral intermediates. In both cases, the rates are encounter-controlled since the progress curves for formation of the complexes are well-described by a simple second-order approach to equilibrium and the rate constants show an inverse solvent viscosity dependence. Assuming that the formation of the intermediate–analogue complex is preceded by an initial ground-state analogue complex, the lifetime of that ground-state complex must be less than ~20 μs. All of the enzyme–inhibitor complexes studied share three characteristics: (1) the complexes generate large UV-difference spectra; (2) a substantial solvent isotope effect is found on the enzyme's affinity for the inhibitors; and (3) a new signal appears in the CD spectra of the complexes. Two of the nucleosides studied, 1-deazapurine riboside and 1-deazaadenosine, form complexes which appear to mimic a ground-state rather than a reactive intermediate when bound to adenosine deaminase. We find that the values for the association rate constants for those inhibitors which form intermediate analogues are very similar to that for adenosine. The presence of a significant solvent isotope effect on the affinity of all inhibitors is attributable in part to a large transfer isotope effect on the free ligand and in part to an effect on the bound ligand. This complicates use of the solvent isotope effect in applications of the multiple isotope method for estimating intrinsic isotope effects and commitment factors.

Adenosine deaminase (EC 3.5.4.4) catalyzes the hydrolysis of (deoxy)adenosine to (deoxy)inosine (Figure 1). Reaction pathways have been proposed (Figure 1) with several discrete chemical intermediates (Wolfenden et al., 1969; Frick et al., 1987; Weiss et al., 1987) or an S_N2 mechanism lacking any stable species on the path from (enzyme-bound) reactants to products (Wilson et al., 1991). Support for a hydrate tetrahedral intermediate has come from studies of alternative substrates (Evans & Wolfenden, 1973), transition-state analogues (Wolfenden et al., 1969), UV-difference spectra (Kurz & Frieden, 1983), and solvent isotope studies (Kurz & Frieden, 1983). ^{13}C NMR studies of the enzyme complex with purine riboside (Kurz & Frieden, 1987; Jones et al., 1989) gave evidence for the formation of an analogue of a tetrahedral intermediate, and that conclusion is now confirmed by the crystal structure of the purine riboside–enzyme complex (Wilson et al., 1991). Thus, with purine riboside, the enzyme catalyzes formation of the tetrahedral intermediate, the first half of an addition–elimination sequence, but is unable to complete turnover owing to its lack of a leaving group at C-6.

In this report, our approach is to use inhibitors that are able to participate in only part of the catalytic cycle in order to isolate and study part of the mechanism without the complication of enzyme turnover. We seek evidence for each of the intermediate species shown in Figure 1. We believe that

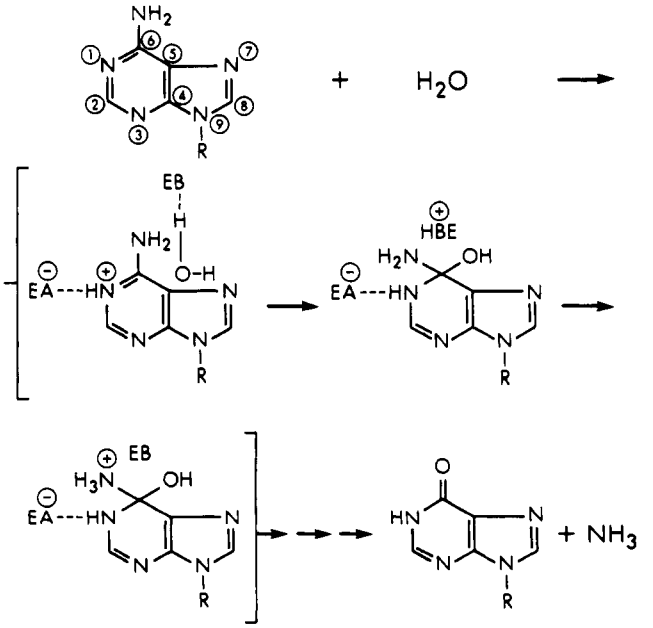

FIGURE 1: Reaction catalyzed by adenosine deaminase including the structures of possible intermediates.

† Supported by National Institutes of Health Grants GM33851 (L. C.K.) and DK13332 (C.F.).

inhibitors lacking N-1 of the purine ring (1-deazanucleosides) form enzyme complexes that are analogues of the ground state rather than the transition state, and we compare their rates of formation to those for inhibitors in the purine series which lack leaving groups (i.e., forming analogues of the tetrahedral intermediate). No evidence is found for a preprotonation intermediate (first structure in brackets of Figure 1) in either series. The progress curves for all inhibitors are well-described as simple second-order approaches to equilibrium. For comparison, we have directly determined the rate constant for the association of adenosine with the enzyme. The second-order rate constants for substrate association and tetrahedral intermediate analogue formation are quantitatively similar.

Materials and Methods

Materials. Adenosine deaminase (calf intestine) was obtained from Sigma Chemical Co. Deoxycoformycin was obtained from Dr. John Douros or Dr. Matthew Suffness of the Developmental Therapeutic Program, National Cancer Institute. 1-Deazapurine and 2,3-diaminopyridine were products of Aldrich Chemical Co. 3-Deazaadenosine was the generous gift of Dr. Gerald Wolberg, Division of Experimental Therapy, Burroughs Wellcome Co.

2-Aminopurine Riboside. This compound was prepared from thioguanosine according to Fox et al. (1958).

1-Deazapurine Riboside. This material was prepared according to Antonini et al. (1984).

1-Deazaadenosine. The synthesis of 1-DAd[1] was a modification of published procedures. Imidazo[4,5-*b*]pyridine was synthesized from 2,3-diaminopyridine according to Antonini et al. (1984). A material more suitable for the next step is obtained if the crude product is recrystallized from 50:50 (v/v) ethanol/heptane. Imidazo[4,5-*b*]pyridine 4-oxide was prepared using *m*-chloroperbenzoic acid as oxidant (Itoh et al., 1982a). Nitration to 7-nitroimidazo[4,5-*b*]pyridine 4-oxide was according to Antonini et al. (1984). Removal of the oxide group to yield 7-nitroimidazo[4,5-*b*]pyridine, formation of the protected ribonucleoside, and its final reduction to 1-DAd followed the procedures outlined by Cristalli et al. (1987). The NH proton of 7-nitroimidazo[4,5-*b*]pyridine is found to resonate at 13.8 ppm in DMSO solution (rather than at the reported 11.1 ppm), the other resonances agreeing with those reported. Deprotection of the *O*-acetyl nucleoside by the procedure described results in large amounts of acetamide contamination which cannot be removed by the recommended chromatographic procedure. Trituration of the sample with a small amount of water removes most of the contaminant. Catalytic hydrogenation proceeds smoothly, but silica gel chromatography (eluant of 85:15 ethyl acetate/methanol) followed by recrystallization from water is required to yield a product with properties agreeing with literature values (Itoh et al., 1982b).

Deoxypurine Riboside. For this compound, we chose any enzymatic route from purine and thymidine using a crude extract of N-deoxyribosyl transferase from *Lactobacillus helviticus* (ATCC 10386) according to Betbeder et al. (1989). After the extraction step, the crude material was chromatographed on a silica gel column eluting with 4:1 ethyl acetate/ethanol. The final product was greater than 95% pure by HPLC.

Enzyme Concentrations. These were determined by active site titration with deoxycoformycin as described elsewhere (Kurz et al., 1985).

Stopped-Flow Experiments. Transient kinetic experiments were performed using an Applied Photophysics stopped-flow spectrophotometer (Model SFMV12) interfaced with an Archimedes 420 Acorn computer and using a 1-cm cell thermostated at 20 °C. Solutions contain 50 mM potassium phosphate and 0.1 mM EDTA, pH(D) 7.50. Wavelengths used to monitor inhibitor binding by absorbance or fluorescence are indicated in the description of data found under Results. Wavelengths used to monitor substrate turnover are 268 nm for adenosine and deoxyadenosine and 248 nm for 2-aminoadenosine. The dead-time of the instrument, an important parameter for fast reactions, was measured using the 5,5′-dithiobis(2-nitrobenzoic acid) thioglycerol reaction (Paul et al., 1980).

UV-Difference Spectroscopy. Difference spectra were obtained at 2-nm resolution using a Hewlett-Packard 8151A diode array spectrophotometer. Identical volumes of ligand and protein solutions (or ligand and acid; exact conditions given in figure legends) were pipetted into each side of stoppered split-compartment cells. After temperature equilibration (20 °C), baseline spectra were recorded. The contents of the cell were mixed, and final spectra were recorded. The spectra obtained before mixing were subtracted from those after mixing, and the result was recorded as the difference spectrum. Dwell times and iterations were set so as to keep standard deviations of the values of the absorbance difference in the region of interest within 1%. With 1-DPR the affinity of the enzyme for the inhibitor is insufficient to ensure complete complex formation at concentrations compatible with acceptable total absorbances. Corrections were applied to the experimental spectra using the dissociation constant of the inhibitor (see Results) in order to generate accurate extinction coefficient values for the reported difference spectra.

Fluorescence. A Spex Fluorolog fluorometer was used for these measurements.

Circular Dichroism (CD). CD spectra were collected from 250 to 300 nm using a Jasco J-600 spectropolarimeter interfaced with an IBM PS2 Model 50 computer. Rectangular cells (10-mm path) or cylindrical cells (1.0-mm path) were thermostated at 20 °C.

Analysis of Progress Curves. Kinetic constants from full time-course data were determined as previously described (Kurz & Frieden, 1983) by fitting progress curves to an appropriate mechanism using the programs KINSIM (Barshop et al., 1983) and FITSIM (Zimmerle & Frieden, 1989). KINSIM allows simulation of progress curve from kinetic mechanisms by numerical integration for comparison with experimental data. FITSIM performs a nonlinear least-squares fit of the simulated progress curve to the experimental data.

Solvent isotope effects on the kinetic constants were measured in the plateau region (pH(D) = 7.50) of their pH(D) dependence as described previously (Kurz & Frieden, 1983). Viscosity effects on kinetic constants were determined (Kurz et al., 1987) using 0.67 M sucrose in standard buffer (η_{rel} = 2.09) as the viscosogenic solvent.

Results

Nucleoside Inhibitor Dissociation Constants and Their Solvent Isotope Effects. Inhibition constants (K_i) (Table I)

[1] Abbreviations: ADA, adenosine deaminase; CD, circular dichroism; 1-DAd, 1-deazaadenosine; dCF, deoxycoformycin; 1-DPR, 1-deazapurine riboside; DHMPR, 1,6-dihydro-6-(hydroxymethyl)purine riboside; $^{D}k_i$ and $^{D}K_j$, solvent isotope effects (the value in H_2O divided by the value in D_2O) on the rate constant k_i and the kinetic constant (or dissociation constant) K_j; $^{s}k_{on}$ and $^{s}k_{off}$, viscosity effects (the value of the rate constant in H_2O divided by the value of the rate constant in a solution containing a viscosogenic solute); DMSO, dimethyl sulfoxide; EDTA, ethylenediaminetetraacetic acid; PR, purine riboside; NHPR, 2-aminopurine riboside.

Table I: Solvent Viscosity and Isotope Effects on the Affinity of Nucleoside Inhibitors for Adenosine Deaminase

nucleoside	$K_i(H_2O)^a$ (μM)	^DK_i (H_2O/D_2O)	^sK_i ratio[b] (η_r = 2.01)
purine riboside	3.77	1.55	0.97[c]
deoxypurine riboside	1.90	1.52	
2-aminopurine riboside	1.89	1.72	0.98
1-deazapurine riboside	26.1	1.58	
1-deazaadenosine[d]	0.180	1.76	1.00
3-deazaadenosine[e]	257	~1.0	

[a] Determined at 20 °C in 50 mM potassium phosphate/1 mM EDTA, pH(D) 7.50. Replicate experiments agree within 5%. [b] Determined in buffer also containing 0.67 M sucrose, η_{rel} = 2.09. [c] Kurz et al. (1987). [d] No change in UV spectrum in presence of ADA for 72 h (this is not a substrate). [e] Changes in UV spectrum in presence of ADA for 72 h are consistent with deamination (this is a poor substrate).

Table II: Kinetic Constants for Alternative Substrates of Adenosine Deaminase

nucleoside	K_m (μM)	K_p (μM)	k_{cat} (s^{-1})	k_{cat}/K_m (μM^{-1} s^{-1})
adenosine	19.2	550	199	10
deoxyadenosine	9.8	176	188	19
2-aminodeoxyadenosine	4.8	40	56	12

for nucleoside competitive inhibitors were determined by fitting simulated progress curves to full time-course data using the mechanism shown in Scheme I (Kurz & Frieden, 1983). The

Scheme I

$$E + S \underset{}{\overset{K_m}{\rightleftharpoons}} ES \xrightarrow{k_{cat}} EP \overset{K_p}{\rightleftharpoons} E + P$$

$$E + I \overset{K_i}{\rightleftharpoons} EI$$

value of K_p in H_2O and D_2O solutions was fixed at a value of 550 μM. This has previously been determined in H_2O solutions by simulation of progress curves for adenosine deamination in the presence of high concentrations of inosine (Kurz & Sharma, unpublished results). In D_2O solutions, K_p is still sufficiently high that the K_i values of inhibitors are insensitive to the value of K_p within wide limits. Values of K_m and k_{cat} were determined from progress curves at low (10 μM) and high (50 μM) adenosine concentrations relative to the K_m value (20 μM). Using these parameters, K_i values were determined from runs at low adenosine levels with sufficient inhibitor to produce approximately 50% inhibition of the initial rate. Table I shows that substantial solvent isotope effects on K_i were observed for all inhibitors.

The inhibition constants (K_i) for nucleoside inhibitors are equilibrium properties and consequently are expected to be independent of solvent viscosity, a dynamic property of the solution. Table I shows that, as in the case of purine riboside (Kurz et al., 1987), the observations for those inhibitors tested are in accord with this expectation.

Kinetic Constants. Values of K_m, k_{cat}, and K_p for deoxyadenosine and 2,6-diaminopurine riboside were determined by simulation (vide supra) of progress curves. However, one additional experiment at very high substrate [(5–10) × K_m] levels was included in order to better define the value of K_p for these substrates. The results are reported in Table II.

Difference Spectra. Figure 2 shows difference spectra for free and bound deazanucleosides, 1-DAd, and 1-DPR, along with that for purine riboside (panel A) compared to the acid-neutral difference spectra (panel B) for those inhibitors. The binding of all three inhibitors to the enzyme results in a large red shift of the wavelength of maximum absorption

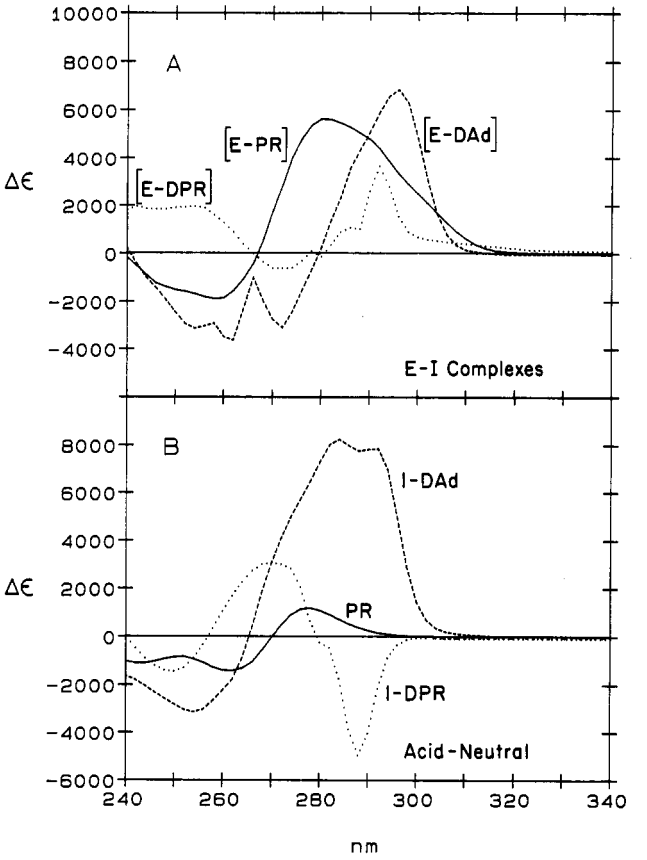

FIGURE 2: (A) Difference spectra for purine riboside (—), 1-deazapurine riboside (···), and 1-deazaadenosine (- - -) bound to adenosine deaminase in 50 mM potassium phosphate/0.2 mM EDTA buffer, pH 7.50, 20 °C. (B) Protonation difference spectra for purine riboside (—), 1-deazapurine riboside (···), and 1-deazaadenosine (- - -) in acid (0.5 M HCl for the first two compounds and 0.1 M HCl for the third) vs neutral solution (20 °C).

compared to the free inhibitor spectrum. Even though 1-DAd contains a 6-amino group and potentially could be deaminated, its difference spectrum is stable for over 72 h, indicating no significant turnover by the enzyme. The spectral changes observed for enzyme complexes (panel A) have little or no resemblance to those which result from protonation (panel B). The protonation difference spectra are found to be stable for at least 20 min, indicating reasonable acid stability. The difference spectrum for the enzyme complex with NHPR also does not resemble the acid-neutral difference spectrum (data not shown).

Figure 3 compares the solvent difference spectra (for solutions of the nucleoside in the indicated solvent vs those in water) for NHPR (panel A) and 1-DAd (panel B) with those generated when these inhibitors bind in the active site. For 1-DAd, the shape and size of the solvent difference spectra are very similar to that for the complex formation, suggesting that environmental factors are affecting the absorption spectrum of the bound inhibitor with no covalent bond changes having taken place. In the case of NHPR [as with other inhibitors of the purine series (data not shown)], there is no similarity between the solvent difference spectra and those for the formation of enzyme complexes. Since 2,6-diaminopurine riboside is a good substrate (Table II) and NHPR is in fact a better inhibitor than purine riboside, the simplest explanation is that the enzyme complex difference spectrum for the NHPR results from formation of a tetrahedral intermediate analogue just as it does in the case of purine riboside.

Circular Dichroism (CD) Spectra. Figure 4 shows the CD spectra from 250 to 350 nm for ADA and the complexes with

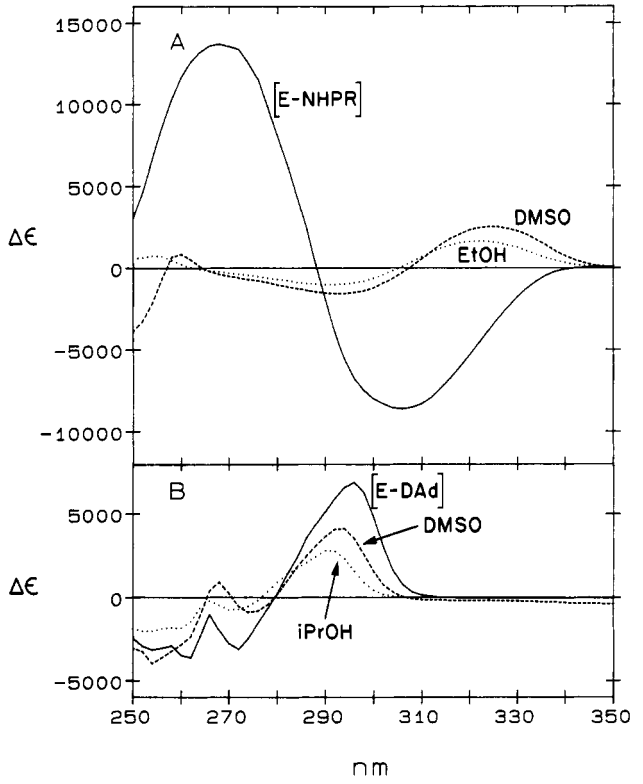

FIGURE 3: (A) Solvent difference spectra for 2-aminopurine riboside in ethanol (···) and DMSO (---) compared to the difference spectrum for the complex with adenosine deaminase (—). (B) Solvent difference spectra for 1-deazaadenosine in 2-propanol (···) and DMSO (---) compared to the difference spectrum for the complex with adenosine deaminase (—).

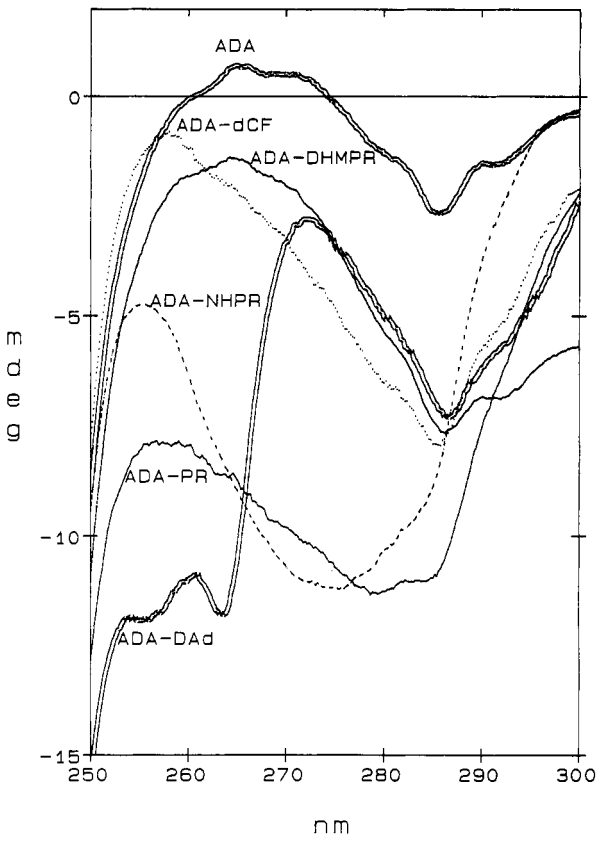

FIGURE 4: CD spectra from 250 to 298 nm for (no ligand) adenosine deaminase (═) and its complexes with dCF (···), DHMPR (—), NHPR (---), PR (—), and DAd (═). Concentrations of enzyme or complex are 17 μM in 50 mM potassium phosphate/0.2 mM EDTA, pH 7.50, 20 °C.

PR, NHPR, 1-DAd, dCF, and DHMPR.

It seems a reasonable expectation that the creation of a new chiral center, as results from hydration of the nucleosides in the active site, could give rise to unique features in their CD spectra. None of the inhibitors with aromatic chromophores have significant CD signals in this region (250–298 nm) in the absence of the enzyme. The transition-state analogue inhibitors, dCF and DHMPR, each of which already has an additional chiral center in the heterocyclic chromophore, have significant positive CD signals (data not shown), which requires corrections to be applied to spectra of enzyme solutions containing excess inhibitor.

All classes of enzyme–inhibitor complexes (after appropriate corrections) show very similar negative CD changes in the region of 285 nm, which appear to be an intensification of the CD signal of the free enzyme in that region. Additional changes for the complexes of the inhibitors are found in the region of their individual maximum absorption. While in the cases of inhibitors which form *new* chiral centers (PR and NHPR) the magnitude of the signal change seems to be somewhat larger, no features of the CD spectra of the enzyme complexes unambiguously distinguish between the transition-state, intermediate-state, or ground state analogues.

Kinetics of Complex Formation. The rates of formation and dissociation of the inhibitor–enzyme complex may be examined either *indirectly* from the inhibitor's effect on the time course of enzyme turnover of substrate or *directly* by monitoring the time course of the spectroscopic signal generated by complex formation.

The indirect method (i.e., using the time course of substrate disappearance) has been used previously to determine the association rate constants for transition-state analogue inhibitors (Frieden et al., 1980). This approach is successful when the association rate constant for the inhibitor is significantly smaller than that of the substrate. For simulation of full time-course data obtained in the presence of inhibitors such as deoxycoformycin, inhibitor binding cannot be described as a rapid equilibrium process (Scheme I) but requires explicit inclusion of the forward and reverse rates for the second-order association step (Scheme II). The indirect method cannot

Scheme II

$$E + I \underset{k_{off}}{\overset{k_{on}}{\rightleftharpoons}} EI$$

be used for inhibitors such as purine riboside or the 1-deazanucleosides because their association rate constants are close to (or faster than) those for adenosine. This is why the mechanism of Scheme I, which treats both substrate and inhibitor binding as equilibrium steps, is adequate to describe the progress curves for competitive inhibititon under multiple-turnover conditions for purine riboside (Kurz & Frieden, 1987) and the 1-deazanucleosides (this work).

If inhibitor affinity is high enough and if a spectroscopic signal of sufficient magnitude accompanies complex formation, then direct determination of the rate of complex formation (in the absence of substrate) is possible. In the case of deoxycoformycin, a transition-state analogue inhibitor, it is possible to apply both the indirect and direct methods. The direct method utilizes the 36% decrease in protein fluorescence which accompanies dCF binding. Both methods yield the same value for the association rate constant. This is of some interest because of conflicting reports in the literature. After an association rate constant of 2 μM^{-1} s^{-1} obtained by the indirect method was reported by Frieden et al. (1980), Philips et al. (1987) reported that the protein fluorescence change accom-

Table III: Second-Order Association and Dissociation Rate Constants for the Binding of Nucleoside Inhibitors to Adenosine Deaminase[a,b]

nucleoside	k_{on} (μM^{-1} s^{-1})	$^{D}k_{on}$	$^{s}K_{on}$	k_{off} (s^{-1})	$^{D}k_{off}$	$^{s}k_{off}$ (η_{rel} = 2.0)
2-aminopurine riboside (λ = 268 nm)	8.9	0.98	1.95	16.8	1.69	1.95
2-aminopurine riboside (λ = 305 nm)[c]	7.3			13.8		
2-aminopurine riboside (fluor λ_{excit} = 305 nm λ_{emiss} > 345 nm)	8.0	0.93		15.2	1.61	
deoxypurine riboside[d] (λ = 280 nm)	8.3			10.4		
1-deazaadenosine (λ = 292 nm)	21.2	1.05	2.1	3.82	1.85	2.1

[a] Day to day variations range from 7 to 10%. Comparisons within a single day agree within 2%. [b] See abbreviations footnote for definitions of $^{D}d_{on}$, $^{s}k_{on}$, etc. [c] It is probable that the differences between rate constants measured under different conditions are not significant. [d] Measured in D_2O. Small $\Delta\epsilon$ values limit conditions for meaningful measurement to D_2O solutions where tighter binding results in a bigger signal.

panying dCF binding to human ADA shows a biphasic time course. We have reexamined this question for the bovine ADA and find no evidence for any rate process other than the expected irreversible second-order one; both methods yield the same value for the association rate constant.

Enzyme–inhibitor complex formation may be followed directly by the change in absorbance at a wavelength where the difference spectrum is of sufficient magnitude (Figures 2 and 3). The data shown in Figure 5 are the absorbance changes resulting from complex formation between ADA and 1-DAd monitored at 292 nm. The progress curve is well-described by a mechanism involving a second-order approach to equilibrium (Scheme II) where the value of the ratio k_{off}/k_{on} is fixed at 0.18 μM, the K_i value obtained from competitive inhibition studies (Scheme I and Table I). Regression analysis of the progress curve[2] yields a value for k_{on} of 21.21 ± 0.03 μM^{-1} s^{-1} (2.1×10^7 M^{-1} s^{-1}).

Rate constants for all the inhibitors were obtained in a similar fashion, and their values are reported in Table III. Replicate measurements yield rate constants which vary from 1 to 10%; those for cases with large signal changes are the more reproducible. In the purine series, the 2-aminopurine difference spectrum is large enough to allow the rate to be followed at either 268 or 305 nm. Values of k_{on} and k_{off} measured at either wavelength are in satisfactory agreement with those measured by following fluorescence quenching (Table III).

In the viscosogenic buffer containing 0.67 M sucrose, η_{rel} = 2.09, second-order approach to equilibrium is again observed, and the rates of formation and dissociation of the complexes are considerably slower; for both 1-DAd and NHPR, there is an approximate 2-fold reduction in the value of k_{on} (Table III).

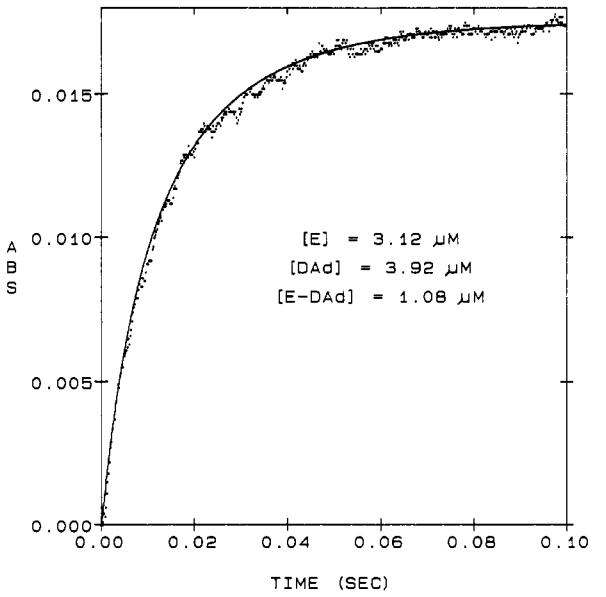

FIGURE 5: Progress curve for formation of the ADA–1-deazaadenosine complex monitored at 292 nm in 50 mM potassium phosphate/200 μM EDTA, pH 7.50, 20 °C. Actual data are represented by the dotted curve. The simulation (solid curve) is for initial concentrations[1] of ADA = 3.12 μM, 1-DAd = 3.92 μM, ADA–DAd complex = 1.08 μM with k_{on} = 21.21 μM^{-1} s^{-1} and k_{off} = 3.818 s^{-1}.

Table IV: Trial of Selected Rate Constants for Two-Step Binding of Nucleoside Inhibitors to Adenosine Deaminase (Scheme III)

k_1 (μM^{-1} s^{-1})	k_2/k_{-2}	k_2 (s^{-1})	$^{s}k_{on}$ (η_{rel} = 2.0)[a]
8	49	56756	1.99
10	49	3356	1.79
14	49	1623	1.56
20	49	1172	1.44
8	19	18264	1.99
20	19	525	1.44

[a] Experimental values of $^{s}k_{on}$ are 1.95 to 2.1 (see Table III).

In reference to Figure 1, the proposed mechanism of the enzyme suggests one or more species on the reaction pathway before the final tetrahedral inhibitor species is formed. At least an initial complex, analogous to the substrate–enzyme ground state, should be present.

A protonated intermediate prior to tetrahedral intermediate formation has been proposed on theoretical grounds (Orosco et al., 1990). Evidence has been presented that an ethenoadenine inhibitor, ϵ-EHNA, is protonated when bound in the active site of ADA (Caiolfa et al., 1990). We have presented data above (solvent and acid-neutral difference spectra) that the spectra of ground-state and protonated intermediates should differ from each other and from that of the final complex and their formation should be experimentally detectable. A kinetically significant intermediate should evidence itself as a lag phase prior to formation of the final complex or as an unexpected initial amplitude change. The magnitude of the additional phase should vary with wavelength in a way

[2] Comment is required on the way in which these data are analyzed. The data are fit from the first correct data point which is given a time of zero. Because our instrument triggers data collection before flow is completely stopped, each data set as collected includes 1.3–1.8 ms before the first correct data point. The data points collected before flow is stopped are routinely omitted from the data set before analysis. Using the thioglycerol test reaction (See Materials and Methods), the first correct data point occurs 1.8 ms after mixing. We will use the formation of the complex with 1-DAd as an example. For this fast reaction, some complex (roughly 25–30% of the total) is formed during the dead-time (1.8 ms) of the apparatus. The actual extent of the *total absorbance change* upon complex formation at equilibrium is measured by subtracting absorbances of appropriate blank runs (absorbances recorded from runs lacking one or both the reactants) from the absorbance after reaction is complete for a kinetic run, (A(ADA+DAd), as shown in the equation

$$\Delta A = A(\text{ADA} + \text{DAd}) - A(\text{buffer} + \text{DAd}) - A(\text{ADA} + \text{buffer}) + A(\text{buffer} + \text{buffer}) = 0.0242 \quad (1)$$

The value so obtained agrees well with that measured in a conventional spectrophotometer (0.0253). Since a smaller absorbance *change*, 0.018, is observed in the kinetic run (ADA + DAd), some complex has been formed before the first correct data point. The consequent reductions in the concentrations of free enzyme and inhibitor are calculated, and the progress curve is then simulated using these new values as initial concentrations.

suggestive of the intermediate's structure.

However contrary to expectation, *no* evidence can be found for more than one kinetic phase (even an initial complex) for any of the inhibitors studied. In all cases, careful measurements of the signal before and after reaction confirm that the portion of the amplitude missed in the dead-time of the stopped-flow spectrophotometer is fully explained by back-extrapolation of the observed second-order process.

Assuming, however, a two-step mechanism for formation of the observed complex in which only the encounter step (k_1 and k_{-1}) is viscosity sensitive (Scheme III), our observations

Scheme III

$$E + I \underset{k_{-1}}{\overset{k_1}{\rightleftharpoons}} EI \underset{k_{-2}}{\overset{k_2}{\rightleftharpoons}} EI'$$

place stringent limits on the values of rate constants. We investigated what steady-state mechanisms involving two steps could accommodate all the data. The NMR spectra of enzyme-bound purine ribose set an upper limit of 4% on the relative concentration of any purine riboside bound to the enzyme and having a chemical shift near that of the free ligand (Kurz & Frieden, 1987) i.e., EI of Scheme III. The value of the ratio, k_2/k_{-2}, is therefore ≥ 24. For any given value of k_1, the value of k_{-1} is equal to $k_1K_i(k_2/k_{-2})$. The only unknowns remaining are the absolute values of k_2 and k_{-2}. For a series of values of k_1, we determined the ranges of values of k_2 that generate progress curves in reasonable agreement with experimental data. For values of $k_1 \geq k_{on}$ (Scheme II), values of k_2 can be found which fit the aqueous solution progress curve. Selected examples are given in Table IV. These values were then used to generate theoretical data sets for a viscous solution with $\eta_{rel} = 2.0$; the values of rate constants k_1 and k_{-1} were divided by 2.0. This progress curve was then fit by the simple second-order mechanism (Scheme II) to give the apparent viscosity dependence of the rate constants k_{on} and k_{off}, ${}^sk_{on}$ and ${}^sk_{off}$. Experimental values of 1.95–2.1 for ${}^s_{kon}$ are found for NHPR and 1-DAd, respectively (Table III). The only two-step cases which are in reasonable agreement with all the data are those in which k_1 has values from 8 to 10 μM^{-1} s^{-1}, close to that of k_{on}. Furthermore, the absolute values of k_2 and k_{-2} required are large; the partition ratio of the initial complex k_2/k_{-1} must exceed a value of 4. Thus, if complex formation occurs in two steps, formation of an initial noncovalent complex followed by an addition reaction forming the tetrahedral intermediate analogue, then the first (encounter) step must be close to rate-determining for intermediate analogue formation. The lifetime of any ground-state–analogue complex cannot be greater than about 20 μs ($1/(k_{-1} + k_2)$).

Single-Turnover Experiments. The direct determination of association and dissociation rate constants for a substrate in a single-substrate enzyme requires the ability to observe the rise to steady state of the enzyme–substrate complex. With the assumptions discussed below, this is now technically feasible for adenosine deaminase. The mechanism used is shown in Scheme IV. Product dissociation is treated essentially as

Scheme IV

$$E + S \underset{k_{-1}}{\overset{k_1}{\rightleftharpoons}} ES \underset{k_{-2}}{\overset{k_2}{\rightleftharpoons}} EP \underset{k_{-3}}{\overset{k_3}{\rightleftharpoons}} E + P$$

an equilibrium step ($k_3 \gg k_{-2}$). Furthermore, $k_3 \gg k_2$ since no significant viscosity dependence on V_{max} is observed. [Viscosity effects on V_{max} are expected when the rate of product dissociation is kinetically significant (Kurz et al., 1987).] The value of $k_3/k_{-3} = K_p$ was fixed at the previously

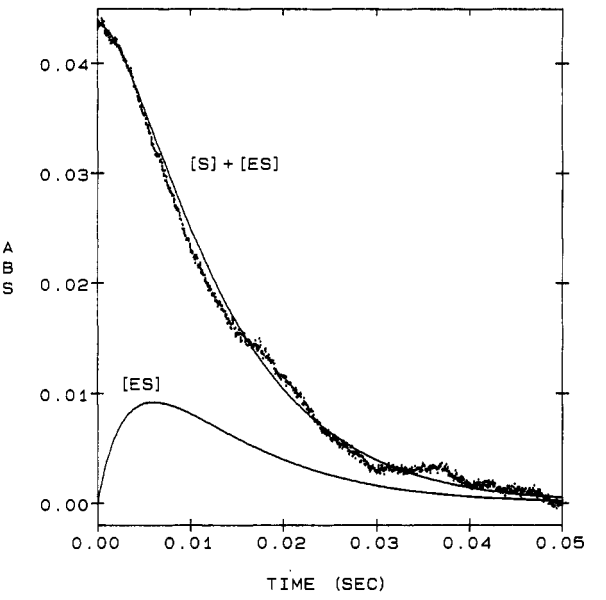

FIGURE 6: Progress curve for deamination of adenosine under single-turnover conditions monitored at 262 nm in 50 mM potassium phosphate/200 μM EDTA, pH 7.5, 20 °C/9.7 μM enzyme/5.6 μM adenosine. Actual data are represented by the dotted curve. The simulation (solid curve) is for the sum of the absorbance of S and ES. The curve labeled [ES] is simulated data for ES alone.

determined (Kurz and Sharma, unpublished results) value of 550 μM. [The only run (vide infra) for which derived k values are sensitive to the value of this parameter is the multiple-turnover experiment at a high adenosine concentration.] This scheme assumes that the chemical transformation (step 2) is irreversible. Under our conditions, the overall scheme is irreversible and we have no evidence for kinetic reversibility. We need to assume that at the wavelength of observation (262 nm) ES and S absorb light equally and also that no intermediate contributes significantly to the absorption changes at this wavelength. Thus, the mechanism treats the turnover of the central complex as a single step ignoring the existence of any chemical intermediates. In our view, these last two (related) assumptions are the most questionable.

Six experiments were performed, and the progress curves were simultaneously fit to this mechanism using KINSIM and FITSIM.[3] Within practical limits, the conditions for the experiments were chosen to maximize the difference between the time courses that would be observed for a mechanism with prior-equilibrium–substrate association versus non-prior-equilibrium conditions: that which would be observed if the rate of substrate association were kinetically significant. Experimental conditions include multiple turnovers at low and high substrate concentration, single turnovers at equimolar enzyme and substrate conditions, and single turnovers with

[3] For the faster reactions (experiments 3–6), the duration of the lag phase (determined by the rise time of the ES complex) in the progress curve is of critical importance in determining the value of k_1. Since these reactions are very fast, a major portion of the lag occurs before the flow is stopped and the dead-time of the instrument is a major concern. By the dead-time we mean the *apparent* age of the solution at the first correct data point, ignoring other issues such as the difference in the age of the solution at the two ends of the cell, etc. From the thioglycerol test reaction (described under Materials and Methods), the first correct data point occurs at 1.8 ms. In contrast to the data for 1-DAd–ADA association, (see footnote 2), the ΔA from this point in the adenosine deamination runs indicates that no significant absorbance change has occurred during this dead-time. Therefore, 1.8 ms of data showing no ΔA are included with the data set prior to the first correct data point and the simulation started at time zero.

enzyme concentrations in excess of that of substrate. The data (dotted curve) from experiment 6 (9.7 μM enzyme and 5.6 μM adenosine) along with the simulated absorbance of E + ES (upper solid curve) obtained from parameters determined by the fit to all six experiments are shown in Figure 6. Also shown in Figure 6 (lower solid curve) is the simulated progress curve for ES alone, illustrating the marked deviation from steady-state conditions for this experiment. The quality of the data for this experiment is the lowest of any member of the series as might be expected from the small total absorbance change (0.043) and short time course (50 ms). The periodic oscillation apparent in the trace is a vibration artifact. The rate constants obtained from the fit to all six data sets are $k_1 = 11.0 \pm 0.4\ \mu M^{-1}\ s^{-1}$, $k_{-1} = 0 \pm 9\ s^{-1}$, and $k_2 = 246 \pm 2\ s^{-1}$. The R-squared value obtained from the regression was 0.998.

Solvent (D_2O) Isotope Effect on the Solubility of Adenosine. The solubility isotope effect for adenosine was measured by preparing saturated solutions in 50 mM potassium phosphate/0.1 mM EDTA, pH(D) = 7.50, 20 °C. The solubility ratio is found to be 1.30 ± 0.05 in favor of the H_2O solution. The chemical potential of the nucleoside in D_2O solutions is significantly higher than in H_2O solutions. This "transfer isotope effect" must be taken into account in the interpretation of any equilibrium or kinetic solvent isotope effects.

Discussion

Structure of 1-Deazanucleosides Bound to ADA. In search of inhibitors which allow study of the structures and rate constants associated with various intermediates, we have prepared 1-DAd and 1-DPR, neither of which is a substrate of adenosine deaminase. Both compounds are competitive inhibitors (Lupidi et al., 1985) with K_i values of 0.2 and 26 μM, respectively. Although both compounds generate large UV-difference spectra upon binding to the enzyme, the difference spectra strongly resemble those obtained from transfer into certain organic solvents, particularly DMSO (Figure 3).[4] Since the difference spectra of the enzyme complexes with 1-deazanucleosides do not resemble the solution acid-neutral difference spectra (Figure 2), protonation of the nucleoside as it occurs in solution is unlikely for the 1-deaza-inhibitors. The most likely explanation is that these inhibitors are ground-state analogues which are not structurally altered as a consequence of binding. Their large UV-difference spectra are then a consequence of the different environment experienced by the chromophore in the active site compared to that in free solution.

The progress curve for binding of 1-DAd to the enzyme is a simple second-order approach to equilibrium, with association and dissociation rate constants inversely proportional to solvent viscosity. The association rate constant, 21 $\mu M^{-1}\ s^{-1}$ is about twice that found for the purine series inhibitors or that of adenosine itself. (Note that using a value of 21 $\mu M^{-1}\ s^{-1}$ for k_1 of Scheme III to fit a two-step mechanism for the *purine* nucleoside inhibitors does *not* yield the observed viscosity dependence.) Interestingly, 1-deazanucleosides show substantial solvent isotope effects on their K_i's and induce CD signals as large as those observed for inhibitors of the purine series that are known to form tetrahedral intermediate–analogues upon complex formation.

In spite of these many similarities to data on the purine nucleosides which form tetrahedral analogues, the 1-deazanucleoside solvent difference spectra indicate that no covalent bond changes are taking place when they are bound to ADA. The large solvent isotope effect on the affinity of these deaza-inhibitors then cannot originate in the hydration of the heterocycle, an explanation previously offered for the solvent isotope effect on the association of the purine series inhibitors (Kurz & Frieden, 1987; Weiss et al., 1987).

Deaza-Inhibitors and the Structure of the Purine Riboside–ADA Complex. 3-DAd is bound at least 10^3-fold more loosely than 1-DAd, a difference of about 4 kcal/mol. On the other hand, 3-DAd is a substrate (albeit a poor one) while the tightly bound 1-DAd is not. The recently published structure of the purine riboside–ADA complex (Wilson et al., 1991) provides both new insights and new questions in connection with the results reported here. Purine riboside hydrate is anchored in the active site by nine hydrogen bonds. N-3 is hydrogen-bonded to an NH of the polypeptide backbone of a glycine residue. N-1 is hydrogen-bonded to a glutamic acid. Our data show that the N-3 interaction is essential for binding but not for catalysis while the N-1 interaction is essential to catalysis but not to binding.

A particularly puzzling aspect of the crystal structure is the lack of any obvious proton donor for the 6-NH_2 of the tetrahedral adduct which would be formed with the actual adenosine substrate. This prompted Wilson et al. (1991) to suggest that the presumptive tetrahedral intermediate is so short-lived as to be essentially nonexistent and to propose an S_N2 mechanism. However, we know that the enzyme can interact with a heterocyclic 6-NH_2 substituent because the affinity of the enzyme for 1-DAd is about 100-fold greater than its affinity for 1-DPR. X-ray structures of the complexes of the deazaadenosine inhibitors would be very useful here.

Interpretation of Isotope Effects. Isotope effects have become major tools in the determination of partition to rate constant ratios for complex enzyme mechanisms and in the determination of transition-state structures where values can be estimated for intrinsic isotope effects on single elementary steps (Cleland, 1982). Both applications have been attempted with adenosine deaminase (Weiss et al., 1987). The formation on the structure of the active site (Wilson et al., 1991) and the new data reported here require a reexamination and reinterpretation of the solvent isotope effects on the interactions of inhibitors and substrates with ADA.

Solvent isotope effects arise when bond force constants involving exchangeable hydrogens have different values in the initial and final states of the system. Conventionally, such effects are discussed in terms of fractionation factors for the relevant hydrogens in the two states (Venkatasubban & Schowen, 1985). A reasonable argument can be constructed that the solvent isotope effects observed for the binding of purine nucleosides to ADA arise from formation of a tetrahedral intermediate (analogue). The expected equilibrium solvent isotope effect for *formation* ($1/^DK$) of the tetrahedral intermediate (last structure in brackets in Figure 1) is given by Φ_r/Φ_{ti} (eq 2) where Φ_r is the product of the fractionation

$$\frac{1}{^DK} = \frac{\Phi_r}{\Phi_{ti}} = \frac{(\Phi_{NH_2})^2(\Phi_{Zn\text{-}H_2O})^2}{(\Phi_{NH_3^+})^3(\Phi_{Zn\text{-}PROH})} \quad (2)$$

factors for exchangeable hydrogens in the reactants and Φ_{ti} is the product of the fractionation factors for the exchangeable hydrogens in the intermediate. The first task is to identify the exchangeable hydrogens that experience changes in their fractionation factors.[5] Then, using model reactions or theo-

[4] Similar solvent difference spectra have been measured for 1-dPR (R. Wolfenden et al., personal communication).

retical calculations, values are assigned to each relevant hydrogen. The fractionation factor for reactants is given by the product of the square of the fractionation factor for the hydrogens of the exocyclic amino group of adenosine and the square of the fractionation factor for the hydrogens in the zinc-bound water. One of these hydrogens remains associated with the zinc-coordinated 6-OH group of the intermediate (analogue). The fractionation factor for the intermediate is given by the product of the cube of the fractionation factor for the protonated amino group of the intermediate and the fractionation factor for the *enzyme-bound* (and zinc-coordinated) hydrated heterocycle. Estimates for these reactant and product fractionation factors are obtained as follows. Values of 0.95 and 1.06 have been determined for the fractionation factors of the hydrogens in $-NH_2$ (adenosine) and $-NH_3^+$ (both amino groups of lysine; Reuben, 1986). The fractionation factor for a free solution hydrated heterocycle, Φ_{PROH}, is closer to 1.00 (Davis & Wolfenden, 1983) than the value, 1.06, the fractionation factor for an alcohol (Rolston & Gale, 1984; Kurz et al., 1986). However, the zinc coordination of this 6-OH suggests that its fractionation factor, $\Phi_{Zn\text{-}PROH}$, should have a value close to that of the zinc-bound water in the initial state. While no values are presently available for zinc, fractionation factors of 0.77–0.72 have been measured (Kassebaum & Silverman, 1989) for the inner coordination water ligands of Co^{2+} in $Co(H_2O)_6^{2+}$ and for two isozymes of Co(II)-substituted carbonic anhydrase. If $\Phi_{Zn\text{-}H_2O} \sim \Phi_{Zn\text{-}PROH} \sim 0.72$, then eq 2 predicts an inverse equilibrium solvent isotope effect of 0.55 for formation of the tetrahedral intermediate. In the absence of a primary solvent isotope effect, this is the maximum kinetic solvent isotope effect value expected for a substrate with rate-determining tetrahedral intermediate formation. For inhibitors lacking a 6-NH_2 substituent, assuming that one hydrogen of the zinc-bound water is transferred to a more normal site, the expected equilibrium solvent isotope effect on the K_i's of the inhibitors forming analogues of the tetrahedral intermediate is approximately 1.4 ($1/\Phi_{Zn\text{-}H_2O}$). These values are reasonably close to those observed experimentally. Weiss et al. (1987) have reported an inverse kinetic solvent isotope effect of $^DV = 0.81$ and $^DV/K = 0.59$ for the alternative ADA substrate, 8-oxoadenosine. We have found solvent isotope effects from 1.5 to 1.8 on the values of K_i for nucleoside inhibitors. For the zinc protease, thermolysin, solvent isotope effects of similar magnitude have been observed on kinetic constants (Izquierdo & Stein, 1990; Stein, 1988) and on the dissociation constant of an inhibitor (R. L. Stein, personal communication, 1990). The isotope effects for thermolysin are argued to arise from transfer of one or more hydrogens of zinc-bound water (where they possess fractionation factors significantly less than one) to sites with more normal values. Given the similarity in active site structures, a similar explanation seems reasonable for ADA.

With ADA however, the situation has added complexity and the simple analysis given above may be significantly flawed. Particularly puzzling is the observation that ground-state analogue inhibitors which do not form tetrahedral intermediate analogues show ^DK_i values as large as those which do. Furthermore, the sensitivity of fractionation factors to specific solvation effects including the details of hydrogen bonding (Kresge et al., 1987) can make a major contribution to kinetic and equilibrium isotope effects. That such solvation effects in the *initial state* (E + I) do make significant contributions to the ADA isotope effects is implied by the observation that solvent isotope effects on the solubilities of nucleosides are surprisingly large, 1.30 for adenosine.

Since $^DK_i = {}^Dk_{off}/{}^Dk_{on}$, we can assess the contribution of such *initial-state* effects to the overall equilibrium effect, ^Dk_i, from our separately measured values of $^Dk_{off}$ ($\sim$1.6–1.8) and $^Dk_{on}$ ($\sim$1.0). Since the binding rate is encounter-controlled and D_2O is 24% more viscous that H_2O (Arnett & McKelvey, 1969), this viscosity difference contributes a factor near 1.24 to both $^Dk_{on}$ and $^Dk_{off}$. Thus, if initial state effects were the *only* contributors to the observed value of ^DK_i ($\sim$1.5–1.8), then $^Dk_{off}$ would be $\simeq$1.24 and $^Dk_{on}$ would be $\simeq 1.24/K_i \simeq$ 0.7–0.8. This clearly is not true (Table III), and we can conclude that effects in the *final state* (enzyme–ligand complex) also contribute significantly. The viscosity-independent factor in $^Dk_{off}$ is 1.4–1.5, and $^Dk_{on}$ is near 1.0 because of a cancellation of the viscosity and initial state effects.

That these *final state* contributions to ^DK_i for the purines can be attributed to one of the originally zinc-bound water protons having been transferred to a more normal site (perhaps N-1) must be questioned, since comparable contributions are present for the 1-deazapurines, which do not form tetrahedral intermediate analogues. At least for the deazapurines, these final-state factors in ^DK_i must arise from *solvation* effects *in the active site*. Alternatively, 1-deazanucleoside inhibitors might bind in a manner that displaces the zinc-bound water. X-ray structures of bound ground-state analogues would be very useful.

Cautionary Note. The apparent large size of the solvation isotope effects for nucleosides is unlikely to be unique to these substances. Many molecules of biological importance participate in multiple hydrogen bonds both in free solution and in enzyme active sites. Any application which utilizes the solvent isotope effect must take these transfer effects into account.

Encounter between Enzyme and Inhibitor Is Rate-Determining for Tetrahedral Intermediate Analogue Formation. Independently of the method of detection, the progress curves for complex formation for all purine analogues show a simple second-order approach to equilibrium. There is no evidence of more than one kinetic phase. The association rate constants for all inhibitors which react to form analogues are similar, 8.3–8.9 μM^{-1} s^{-1}, with the differences in affinity mainly reflected in the *dissociation* rate constants. Most importantly, both association and dissociation rate constants are found to be inversely proportional to the solvent viscosity. This result argues against a kinetically significant prior-equilibrium complex formed before reaction to form the tetrahedral intermediate analogue. Further, only two-step steady-state mechanisms with rate constant values such that the encounter step is primarily rate-determining for intermediate analogue formation are compatible with the overall equilibrium constant and the progress curves for both aqueous and viscous solutions. The most parsimonious explanation is that intermediate analogue formation is sufficiently fast that the encounter is rate-determining and the solvent isotope effects observed are a consequence of the transfer of the ligand from water (H_2O or D_2O) into another solvent (the other "solvent" in the present case being the active site).

[5] In addition to the active site Zn, the active site of ADA contains several potential catalytic residues which might have exchangeable hydrogens with fractionation factors whose values could conceivably change upon tetrahedral intermediate formation. However, these are all oxygen (Asp) and nitrogen (His) sites (Wilson et al., 1991), which in the absence of unusual effects typically should have fractionation factors values very close to 1.0. Further information on the contribution of these residues might be gained through study of the impact of changes in these residues on the magnitude of the solvent isotope effect.

Alternative Explanations. Mechanisms involving an enzyme conformation change and/or displacement of specifically bound water from the active site crevice can be constructed that explain both the viscosity-dependent kinetics and the solvent isotope effects for all classes of inhibitors.

These other explanations must deal primarily with the viscosity dependence of the process. Interestingly, *preformed* tetrahedral transition-state analogues such as dCF and DHMPR also associate with the enzyme in an apparent second-order process with the expected inverse viscosity dependence. In these cases however, the magnitudes of the second-order rate constants are from one to several orders of magnitude lower than the values reported here for nucleosides which *form* analogues after they are in the active site.

We have previously suggested (Kurz et al., 1987) that a diffusion-limited rate-controlling enzyme conformation change is responsible for both the low absolute magnitude and viscosity dependence of the rate constants for association of transition-state analogue inhibitors with adenosine deaminase. Large conformation changes must take place upon tetrahedral analogue formation as indicated by the almost complete solvent inaccessibility shown by purine riboside hydrate in the recently reported X-ray structure of its complex with ADA (Wilson et al., 1991). A reaction requiring movement of a large protein segment will exhibit the viscosity dependence of that motion. This mechanism implies that the active site is initially complementary to the ground-state and that some difficulty is encountered in rearranging the active site in order to accommodate an (imperfect) analogue of the transition state. Apparently, accommodation of the real transition state (intermediate) is much easier.

Another related mechanism has been suggested by Bartlett and Marlowe (1987) to explain the slow binding and viscosity dependence (Bartlett et al., 1988) of rate constants for binding of transition-state analogue inhibitors to thermolysin. They propose that transition-state analogue inhibitor binding requires the displacement of a specific water molecule(s) from the active site. If the concentration of enzyme molecules lacking the specific water is sufficiently low, then the value of the association rate constant may be significantly smaller than that usually expected for such an encounter-controlled process. It is tempting to implicate the zinc-bound water. For ADA, this explanation is attractive since the viscosity-dependent rates of complex formation with the transition-state analogue inhibitors (dCF and DHMPR) are significantly less than those with inhibitors which form intermediate analogues *after* they are bound in the active site. This would be reasonable if transition-state analogue inhibitors required the prior *loss* of the zinc-bound water while 6-H-purine substrate analogues *utilize* it to form intermediate analogues. In its simplest form, this "rare" enzyme species mechanism would predict that all transition-state analogue inhibitors should associate with the enzyme with the same apparent second-order rate constant. However, these values vary ~20-fold (Frieden et al., 1980; Kurz et al., 1987). One possible explanation is that only one (or a few) of many possible encounter complexes is (are) capable for proceeding on to the ligand–enzyme complex. The abortive, nonreactive nature of most of the complexes could result from incorrect orientation on incorrect local enzyme conformation. We note that the tightest binding inhibitors (the higher affinity perhaps monitoring the effectiveness of short-range forces) have the fastest apparent association rate constants.

The dissociation constants for transition-state analogue inhibitors from ADA also show significant solvent isotope effects. It is likely that the –OH moiety of transition-state analogue inhibitors coordinate to zinc since this particular interaction is clearly important for the extremely high affinity of the enzyme for purine riboside hydrate (Wilson et al., 1991). Displacement of the zinc-bound water by transition-state analogue inhibitors then results in a net loss of one hydrogen with a low fractionation factor, generating the observed solvent isotope effect.

Stickiness of Adenosine. A "sticky" substrate is one which, when bound to the enzyme partitions forward to products more often than it dissociates backward to reactants (Cleland, 1986). Two indirect methods have previously been used to determine the stickiness of adenosine to ADA. These two methods give conflicting results. Using the viscosity variation method, Kurz et al. (1987) have presented data indicating that the bimolecular reaction rate (V_{max}/K_m) is entirely encounter-controlled and that the partition ratio (k_2/k_{-1}) is very large (i.e., the substrate is sticky). On the other hand, using the shape of plots of ($V_{max}/K_m)K_i$ vs pH as a criterion for the stickiness of a substrate, Weiss et al. (1987) concluded that adenosine is not sticky and that free enzyme, substrate, and enzyme–substrate complex levels are maintained at their equilibrium values. Both of these methods rely upon analysis of the response of the enzyme-catalyzed reaction rate to the application of a perturbation: the presence of a viscosogenic agent or a change in pH, respectively. Although appropriate controls were done in both cases, the possibility always exists that the kinetic mechanism changes in the presence of the perturbant. Thus, an opportunity exists for misleading results. The results of single-turnover experiments, yielding a more direct measure of the value of the rate constant for substrate association, can resolve this issue.

The value of k_1 for adenosine, 11 μM^{-1} s^{-1}, determined from fitting the six progress curves to the mechanism of Scheme IV, agrees with the value of k_1, 11 μM^{-1} s^{-1}, determined using the viscosity variation method (Kurz et al., 1987). The exact value of k_{-1} could not be determined from our data. Assuming k_{-1} to have a value of 10 (1 standard deviation above zero), adenosine partitions forward to products greater than 25 times more often than it dissociates backward to reactants. Therefore, adenosine is very sticky.

Is Encounter between Enzyme and Substrate Rate-Determining for Tetrahedral Intermediate Formation? Noting the similarity in the values of the apparent rate constants for formation of intermediate analogues with the value of the association rate constant for adenosine (vide supra), it seems reasonable to propose that for adenosine deaminase the formation of intermediates in the reaction of the natural substrate, adenosine, is also very fast. However, the lack of a leaving group is not the only difference between the 6-H-purine inhibitors and actual 6-NH_2 substrates of the enzyme. The exocyclic amino group of the base is part of the aromatic system of the heterocycle and the C-6–N bond has a bond order near 1.5 (Saenger, 1988). Loss of this resonance energy as a consequence of tetrahedral intermediate formation might make the formation of that intermediate more difficult (and perhaps slower) than in the case of the 6-H bases. This difference should be offset to some degree by the greater aromatic delocalization within the ring itself shown by the 6-H compounds (Takeda et al., 1974). Conservatively, the rate of formation of 6-H tetrahedral analogues may be regarded as an upper limit on the rate of formation of the actual 6-NH_2 intermediate.

With the recent determination of the structure of the ADA–purine riboside complex (Wilson et al., 1991), the

construction of mutants in active site residues has become possible. We expect that such mutants or the equally interesting metal-substituted enzymes will allow us, using the techniques described in this work, to successfully detect and characterize the reaction intermediates or alternatively support the unexpected S_N2 pathway.

ACKNOWLEDGMENTS

We thank Dr. Frederick Rudolph (Rice University), whose comment regarding the high rate of deamination of 2-aminoadenosine catalyzed by ADA prompted us to examine NHPR as a tetrahedral intermediate analogue.

REFERENCES

Antonini, I., Cristalli, G., Franchetti, P., Grifantini, M., Martelli, S., & Petrelli, F. (1984) *J. Pharm. Sci. 73*, 366.

Arnett, E. M., & McKelvey, D. R. (1969) in *Solute–Solvent Interactions* (Coetzee, J. F., & Ritchie, C. D., Eds.) p 347, Dekker, New York.

Barshop, B. A., Wrenn, R. F., & Frieden, C. (1983) *Anal. Biochem. 130*, 134.

Bartlett, P. A., & Marlowe, C. K. (1987) *Biochemistry 26*, 8553.

Bartlett, P. A., Drewry, D. H., Hanson, J. E., & Marlowe, C. K. (1988) in *Peptides: Chemistry and Biology, Proceedings of the 10th American Peptide Symposium* (Marshall, G. A., Ed.) p 431, ESCOM Science Publishers, Leiden, The Netherlands.

Betbeder, D., Hutchinson, D. W., Richards, O'L. A. (1989) *Nucleic Acids Res. 17*, 4217.

Caiolfa, V. R., Gill, D., & Parola, A. H. (1990) *FEBS Lett. 260*, 19.

Cleland, W. W. (1982) *CRC Crit. Rev. Biochem. 13*, 385.

Cleland, W. W. (1986) in *Investigation of Rates and Mechanisms of Reactions* (Bernasconi, C., Ed.) Vol. 6, p 791, Wiley, New York.

Cristalli, G., Franchetti, P., Grifantini, M., Vittori, S., Bordoni, T., & Geroni, C. (1987) *J. Med. Chem. 30*, 1686.

Davis, K. R., & Wolfenden, R. (1983) *J. Org. Chem. 48*, 2280.

Evans, B. E., & Wolfenden, R. (1973) *Biochemistry 12*, 392.

Fox, J. J., Wempen, I., & Hampton, A. (1958) *J. Am. Chem. Soc. 80*, 1669.

Frick, L., Neela, J. P. M., & Wolfenden, R. (1987) *Bioor. Chem. 15*, 100.

Frieden, C., Jurz, L. C., & Gilbert, H. R. (1980) *Biochemistry 19*, 5303.

Itoh, T., Ono, K., Sugawara, T., & Mizuno, Y. (1982a) *J. Heterocycl. Chem. 19*, 513.

Itoh, T., Sugwara, T., & Mizuno, Y. (1982b) *Heterocycles 17*, 305.

Izquierdo, M. C., & Stein, R. L. (1990) *J. Am. Chem. Soc. 112*, 605.

Jones, W., Kurz, L. C., & Wolfenden, R. (1989) *Biochemistry 28*, 1242.

Kassebaum, J. W., & Silverman, D. N. (1989) *J. Am. Chem. Soc. 111*, 2691.

Kati, W. M., & Wolfenden, R. (1989) *Science 243*, 1591.

Kresge, A. J., Moore O'Ferrall, R. A., & Powell, M. F. (1987) in *Isotopes in Organic Chemistry, Vol. 7, Secondary and Solvent Isotope Effects* (Buncel, E. & Lee, C. C., Eds.) p 177, Elsevier, New York.

Kurz, L. C., & Frieden, C. (1983) *Biochemistry 22*, 382.

Kurz, L. C., & Frieden, C. (1987) *Biochemistry 26*, 8450.

Kurz, L. C., LaZard, D., & Frieden, C. (1985) *Biochemistry 24*, 1342.

Kurz, L. C., Weitkamp, E., & Frieden, C. (1987) *Biochemistry 26*, 3027.

Lupidi, G., Cristalli, G., Marmocchi, F., Riva, F., & Grifantini, M. (1985) *J. Enzyme Inhib. 1*, 67.

Orozco, M., Canela, E. I., & Franco, R. (1990) *Eur. J. Biochem. 188*, 155.

Paul, C., Kirschiner, K., & Haenisch, G. (1980) *Anal. Biochem. 101*, 442.

Philips, A. V., Robbins, D. J., Coleman, M. S., & Barkley, M. D. (1987) *Biochemistry 26*, 2893.

Reuben, H. (1986) *J. Am. Chem. Soc. 108*, 1082.

Rolston, J. H., & Gale, K. L. (1984) *J. Phys. Chem. 88*, 4394.

Saenger, W. (1988) in *Principles of Nucleic Acid Structure*, p 53f, Springer-Verlag, New York.

Stein, R. L. (1988) *J. Am. Chem. Soc. 110*, 1988.

Takeda, T., Ohashi, Y., & Sasada, Y. (1974) *Acta Crystallogr. B30*, 825.

Venkatasubban, K. S., & Schowen, R. L. (1985) *CRC Crit. Rev. Biochem. 17*, 1.

Weiss, P. M., Cook, P. F., Hermes, J. D., & Cleland, W. W. (1987) *Biochemistry 26*, 7378.

Wilson, D. K., Rudolph, F. B., & Quiocho, F. A. (1991) *Science 252*, 1278.

Wolfenden, R. (1972) *Acc. Chem. Res. 5*, 10–18.

Wolfenden, R., Wentworth, D. F., & Mitchell, G. N. (1969) *Biochemistry 16*, 1571.

Zimmerle, C. T., & Frieden, C. (1989) *Biochem. J. 258*, 381.